SLAC-TN-07-015

August 2007

Definition of a Twelve-Point Polygonal SAA Boundary for the GLAST Mission

Sabra I. Djomehri

Office of Science, SULI Program 2007

University of California, Santa Cruz

Stanford Linear Accelerator Center

Menlo Park, California

August 24, 2007

Prepared in fulfillment of the requirement of the Office of Science, Department of Energy's Science Undergraduate Laboratory Internship under the direction of Markus M. Ackermann at the Kavli Institute for Particle Astrophysics at Stanford Linear Accelerator Center.

Participant: _____
Signature

Research Advisor: _____
Signature

Work supported in part by US Department of Energy contract DE-AC02-76SF00515

TABLE OF CONTENTS

I. ABSTRACT

Definition of a Twelve-Point Polygonal SAA Boundary for the GLAST Mission. SABRA I. DJOMEHRI (University of California, Santa Cruz, CA 95064) MARKUS M. ACKERMANN (Stanford Linear Accelerator Center, Menlo Park, CA 94025).

The Gamma-Ray Large Area Space Telescope (GLAST), set to launch in early 2008, detects gamma rays within a huge energy range of 100 MeV – 300 GeV. Background cosmic radiation interferes with such detection resulting in confusion over distinguishing cosmic from gamma rays encountered. This quandary is resolved by encasing GLAST's Large Area Telescope (LAT) with an Anti-Coincidence Detector (ACD), a device which identifies and vetoes charged particles. The ACD accomplishes this through plastic scintillator tiles; when cosmic rays strike, photons produced induce currents in Photomulitplier Tubes (PMTs) attached to these tiles. However, as GLAST orbits Earth at altitudes ~550km and latitudes between -26° and 26°, it will confront the South Atlantic Anomaly (SAA), a region of high particle flux caused by trapped radiation in the geomagnetic field. Since the SAA flux would degrade the sensitivity of the ACD's PMTs over time, a determined boundary enclosing this region need be attained, signaling when to lower the voltage on the PMTs as a protective measure. The operational constraints on such a boundary require a convex SAA polygon with twelve edges, whose area is minimal ensuring GLAST has maximum observation time. The AP8 and PSB97 models describing the behavior of trapped radiation were used in analyzing the SAA and defining a convex SAA boundary of twelve sides. The smallest possible boundary was found to cover 14.58% of GLAST's observation time. Further analysis of defining a boundary safety margin to account for inaccuracies in the models reveals if the total SAA

hull area is increased by ~20%, the loss of total observational area is < 5%. These twelve coordinates defining the SAA flux region are ready for implementation by the GLAST satellite.

II. INTRODUCTION

The universe contains a myriad of exotic entities, some able to produce enormous amounts of energy. Gamma-ray radiation, generated by such objects as black holes, neutron stars, and relativistic hot gas, is the most energetic form of radiation. The Gamma-ray Large Area Space Telescope (GLAST) seeks to unravel mysteries behind such extraordinary phenomena in order to better understand the high-energy world and how it affects the behavior of the universe. Set to launch in early 2008, the GLAST satellite is highly sensitive to gamma rays within an approximate energy range of 100MeV-300GeV [1]. Being 30-100 times more sensitive than any previous gamma ray telescope, GLAST aims at locating gamma ray sources throughout the universe and studying their properties [1].

A key component of GLAST is its outer detector layer, called the Anti-Coincidence Detector (ACD), whose purpose is to efficiently identify and disregard incident charged particles. In order to maximize its veto capabilities, the ACD consists of 89 plastic scintillator tiles, for which signals produced in them are read out by Photomultiplier Tubes (PMTs) [2]. When the scintillators encounter an influx of charged particles, photons are produced which pass into the PMT. Upon entering, the photons encounter the photocathode, causing electrons to be ejected via the photoelectric effect. These electrons proceed towards an increasingly positive series of dynodes, generating a

cascade of electrons [3]. This amplification of electrons generates a measurable current which indicates when an "unwanted" particle has been received by the ACD. About its orbit, GLAST will encounter many such charged particles; the particles of greatest concern to GLAST are those that have been captured by the geomagnetic field.

Earth's magnetic field acts as a shield from solar and cosmic particles, either by deflecting or trapping them. When such energetically charged particles become trapped, their movement is controlled by the magnetospheric magnetic field and the aggregate of particles forms regions above Earth known as the inner and outer Van Allen radiation belts. The trajectory of a trapped particle residing in these belts is described by gyration along magnetic field lines and gradual longitudinal drifts westward or eastward (for ions or electrons, respectively) [4]. The toroidal surfaces generated from this kind of motion are called drift shells. In order to describe the behavior of trapped radiation, the McIlwain coordinate system for dipole/non-dipole situations can be applied. This system identifies the coordinates (B,L) , for which B represents the relative magnetic field intensity with respect to the magnetic equator, and L signifies the equatorial radius of a drift shell [4]. It is important to note that a particle always remains on the same drift shell, which is different than a magnetic shell. A unique effect of the characteristic properties of the geomagnetic field is a phenomenon called the South Atlantic Anomaly (SAA), a portion of the inner Van Allen radiation belt that approaches closest to the Earth’s surface.

A common problem affecting satellites (and in particular GLAST's ACD) occurs when their orbit crosses the SAA. At this altitude, the flux of radiation is significantly higher than anywhere else due to both the offset center of the geomagnetic field and its tilt from Earth’s axis [5]. Passing through this high radiation environment degrades the

sensitivity and thus performance of the ACD by inducing high currents in the PMTs. To prevent this, the ACD must be turned off from survey mode when it encounters the SAA zone, which contributes to lost observation time. In order to maximize GLAST's period of observation, precision is necessary in determining the smallest possible polygonal boundary of the SAA region.

III. MATERIALS AND METHODS

a) Models

To determine the SAA boundary region for GLAST, models of trapped radiation are applied. The standard models of radiation belt energetic particles are the AP-8 and AE-8 models, for protons and electrons, respectively. These models produce omnidirectional fluxes as functions of the geomagnetic coordinates, B/B_o and L, where $B_o = 0.311653/L^3$ [6]. They map fluxes in the energy range 0.04 MeV - 7 MeV for electrons and 0.1 MeV - 400 MeV for protons. Being able to cover this energy range is a significant improvement from older AP models (i.e. AP-1,5,6, and 7), which contain large discrepancies in the energy spectra [7]. Another feature of this model is that it can describe solar maximum/minimum cycles; however, time variations beyond solar cycles are not considered. All data is taken from nearly two dozen satellites from the sixties and seventies [7].

In addition to the standard model, the PSB97 model is also used. This model specifically maps low altitude proton fluxes in the energy range between 18 MeV - 500 MeV, and is restricted to fluxes during solar minimum conditions [8]. Data for this model is taken from the SAMPEX satellite. Geomagnetic field models are necessary to translate

geographical coordinates of fluxes into geomagnetic coordinates. For that purpose, the IGRF-10 is used throughout this work [9]. However, since the population of high-energy charged particles (> 10 MeV) stably trapped by the geomagnetic field mainly consists of protons, most of the energy acquired by GLAST's ACD is due to protons. Therefore, the following investigation is restricted to SAA proton fluxes.

b) Operational Constraints

As such models can be used to provide visuals of the approximate boundary of the SAA, they do not actually calculate a boundary of the type required by GLAST. The GLAST requires all enclosing edges of this boundary region to be convex to prevent passing through the SAA more than once per orbit. In order to do this, one must calculate the convex hull of the SAA region. A convex hull is the smallest convex set that includes a given set of points [10]. Figure 1 represents a 3D convex hull, where the overall shape is determined by the extreme (or outer) points in the set [11]. For the purpose of attaining the SAA boundary, simply finding a 2D hull of the SAA is necessary. Python scripts evaluate all points in a grid of latitudes (-26°, 26°) and longitudes (-180°, 180°) that have fluxes larger than 1 particle/(cm^2 s), and places these points in a set for determining the convex hull. In addition to being convex, another technical requirement for this polygon is that it must have twelve edges.

c) The Algorithm

Various convex hull algorithms have been produced, some faster than others. Examples of some well known algorithms include Graham Scan (in O($n$log$n$) time), QuickHull (in O(nk) time), and Brute Force (in O(n^4) time) [12]. The time described here represents the number of operations utilized by an algorithm to solve the given problem,

with n being the number of points in the input set, and k being the number of vertices on the output hull. The less factors existing, the shorter the runtime resulting in a faster algorithm. The fairly quick and simplistic algorithm, QuickHull, is used in this work to determine the SAA's convex hull. Its basic procedure is generating a full hull by first calculating an upper and lower hull. QuickHull does this by using triangulation; it starts by finding the leftmost highest and rightmost lowest extreme points (a,b), finds a third extreme point c farthest away from ab (in the orthogonal direction), discards all points inside Δabc, and then recurses on the sides (a,c) and (c,b). Figure 2 is a representation of this procedure [12].

IV. RESULTS

Before the actual convex hull is attained, it is necessary to test the accuracy of the two available models (AP8 and PSB97). Figure 3 shows two possible versions of the SAA flux region as defined by both models in the year 2008; the gray contour representing the AP8 SAA and the blue contour lines describing the PSB97 SAA. In all following contour graphs presented, only protons with energies larger than 20 MeV are considered, and all fluxes (shown by the colorbars) given in particles/(cm^2 s) correspond to a logarithmic scale of base 10. Since both SAA representations are valid, the determined SAA boundary should encompass both resulting in a type of combined hull.

Two concerns that must be considered when defining this boundary are the disparities at solar maximum/minimum conditions and those that arise after extended time periods. Figure 4 compares changes in the SAA at solar minimum and solar maximum using the AP8 model, with the gray contour representing solar minimum

conditions and the blue contour lines defining the solar maximum situation. At solar maximum, the size of the SAA is predicted to decrease due to increased particle interaction with the Earth's upper atmosphere. These interactions cause erosion of the SAA's outer edges, whose effects are verified by Figure 4. Since the flux region at solar maximum never expands past the solar minimum flux region, this factor is ignored in defining the SAA boundary and thus is no longer a concern.

Another potential concern regards shifts in the SAA over large temporal intervals. As mentioned above, protons have a slow longitudinal westward drift, which is a ~0.3° shift per year [4]. Figure 5 verifies this shift, and reveals how slight the shift actually is even over the course of a decade. The gray contour represents the AP8 model in the year 2000, while the blue contour lines describe the AP8 model in the year 2010. Since this westward shift is relatively unsubstantial, it can also be ignored when defining the SAA hull (assuming periodic updates of the boundary's coordinates are implemented).

The next three figures, Figures 6-8, exemplify the evolution of the defined SAA boundary from an *n*-sided polygon to the desired 12-sided polygon. To account for uncertainties in the models, each point with a flux > 1 particle/(cm^2 s) in either the two models is considered inside the SAA. Each point on a densely spaced grid of latitudes and longitudes is classified based on this condition as lying inside or outside the SAA and the convex hull enclosing all inner points is calculated by the QuickHull algorithm.

Figure 6 shows an attained *n*-sided polygon defined by the blue line, which encloses the green region containing all points in the SAA with fluxes > 1 particle/(cm^2 s). Figure 7 compares the previously attained *n*-sided convex hull from Figure 6 with the reduced 12-sided convex polygon. To achieve this reduction, the area loss is < 0.01%,

which signifies that the technical requirement of the GLAST to be bounded by a 12-edge polygon does not decrease GLAST's total observational time by any substantial amount. Figure 8 compares the newly attained 12-edge convex SAA boundary with the original SAA flux regions of both models, where the red line is the defined boundary, the gray contour represents fluxes corresponding to the AP8 model, and the blue contour lines once again show fluxes corresponding to the PSB97 model. The figure verifies that the determined SAA hull actually envelopes both models' SAA representations, and displays twelve coordinate points which accurately define the vertices of the SAA polygon. (See Table 1 for exact coordinates).

One safety measure that can be applied to account for uncertainties in these models' predictions is determining a suitable margin of error for this boundary. Again, python scripts were used in developing scaled versions of the SAA polygon. An example can be seen in Figure 9, which shows the possibility of an SAA hull expanded in all directions (except the hull's base) by 3°. Table 1 compares the twelve unscaled vertices of the SAA polygon with the twelve SAA vertices scaled by 1°, 3°, and 5°. The impact of having such a safety margin can be further analyzed from Table 2, which gives a range of scaled amounts, from 0.5° – 5°. For example, if the SAA polygon were actually to be scaled by 3°, this would account for an increase in SAA area by ~13%, but the total loss in observational time (measured by the loss in observational area) would be roughly 2.25%. Even if the SAA boundary were scaled by 5°, which would increase the area by ~22%, the loss of observational time is still comfortably < 5%.

V. DISCUSSION AND CONCLUSIONS

The objective of this project was to meticulously define a 12-edge convex SAA polygonal boundary of minimum area in order to ensure maximum observational time for GLAST. The vertices defining this polygon are noted in Table 1. By utilizing these coordinates in its software, GLAST will know when to lower the voltages of the ACD and thus when it should be shut off from survey mode during the time spent crossing over the SAA high flux zone. This will ensure lasting efficiency of the ACD, which itself strives to protect and support efficiency of GLAST's ability to take data.

Coordinates revealed above were derived based on the operational constraints of GLAST to have a polygonal boundary with twelve sides, be convex, and only consider latitudes of (-26°, 26°) and longitudes of (-180°, 180°). Conditions at solar maximum did not affect the definition of this boundary, nor did large spans of time; these concerns were left behind when the convex hull was actually determined. After an *n*-sided SAA polygon was defined using the AP8/PSB97 trapped radiation models and the QuickHull algorithm, a concern arose regarding a potentially considerable loss in observational area when the hull is reduced from *n* sides to twelve. However, this concern is quelled by the fact that twelve edges can be almost directly drawn on top of the *n*-edged polygon, resulting in a total observational area loss of < 0.01%. The determined SAA boundary of minimum area was found to cover 14.58% of GLAST's observation time. Further analysis entails deciding an appropriate safety margin for the SAA boundary due to possible errors within the models. Results show that scaling the SAA polygon by 0.5° – 5° can increase polygonal area in a range between ~ 2% - 22%. However, for this range of scaling,

GLAST's total observational time decreases by < 5%, or more specifically by ~ 0.35% - 3.8%.

VI. ACKNOWLEDGMENTS

This research was supported by the Kavli Institute for Particle Astrophysics at Stanford Linear Accelerator Center, Department of Energy, Office of Science. I would like to thank my mentor Markus Ackermann, Greg Madejski, and Doug Applegate for all their support and assistance throughout the term of my internship. Also, I would like to thank the Department of Energy, the Office of Science, and the SULI Program for providing my participation in this sublime internship experience.

VII. REFERENCES

[1] Michelson, P.F. "Instrumentation for the Gamma-ray Large Area Space Telescope (GLAST) mission," X-Ray and Gamma-Ray Telescopes and Instruments for Astronomy, vol. 4851, pp. 1144-1150, 2003.

[2] Moiseev, A.A., Hartman, R.C., Johnson, T.E., Ormes, J.F., Thompson, D.J., "Design and Characteristics of the Anticoincidence Detector for the GLASTE Large Area Telescope," Proceedings of the 29th ICRC, Pune, India, 2005.

[3] Tissue, B.M., "Photomultiplier Tube", [Online document], 1996 Feb 21, [cited 2007 July 3], Available http: http://elchem.kaist.ac.kr/vt/chem-ed/optics/detector/pmt.htm

[4] McIlwain, C. E., Coordinates for Mapping the Distribution of Magnetically Trapped Particles, *J. Geophys. Res., 66*, 3681-3691, 1961.

[5] Daly, E.J., "The Radiation Belts", in Radiation Physics and Chemistry, 43, 1, pp.1-18 (in Special Issue on Space Radiation Environment and Effects), 1994.

[6] Hess, W.N., The Radiation Belt and Magnetosphere, Blaisdell Publ. Co., 1968.

[7] Heynderickx, D., J. Lemaire, E. J. Daly, and H. D. R. Evans, Calculating Low-Altitude Trapped Particle Fluxes With the NASA Models AP-8 and AE-8, *Radiat. Meas., 26*, 947-952, 1996b.

[8] Heynderickx, D., M. Kruglanski, V. Pierrard, J. Lemaire, M. D. Looper, and J. B. Blake, A Low Altitude Trapped Proton Model for Solar Minimum Conditions Based on SAMPEX/PET Data, *IEEE Trans. Nucl. Sci., 46*, 1475, 1999.

[9] The International Association of Geomagnetism and Aeronomy, IAGA, "The International Geomagnetic Reference Field (IGRF)", [Online reference guide], 2007, [cited 2007 July 23], Available http: www.iugg.org/IAGA/iaga_pages/pubs_prods/**igrf**.htm

[10] Computer Science Dept., Stony Brook Univ., "Convex Hull", [Online Resource], 2001 Mar 7, [cited 2007 July 18], Available http: www.cs.sunysb.edu/~algorith/files/**convex-hull**.shtml

[11] xCellerator, ConvexHull, California Institute of Technology, 2005, [cited 2007 July 23], Available http: http://xlr8r.info/mPower/pages/convexHull.html

[12] O'Rourke, J. Computational Geometry in C. 2nd Ed., Cambridge University Press, 1998.

VIII. FIGURES

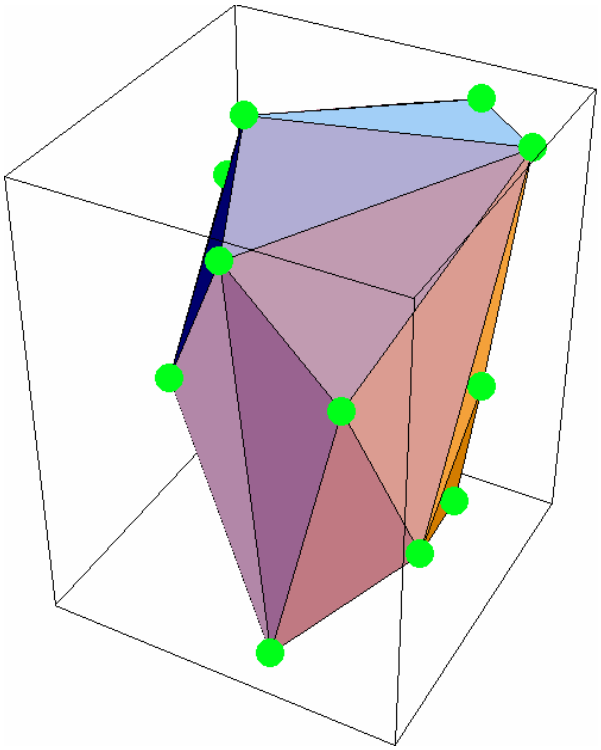

Figure 1. Three-dimensional representation of a convex hull.

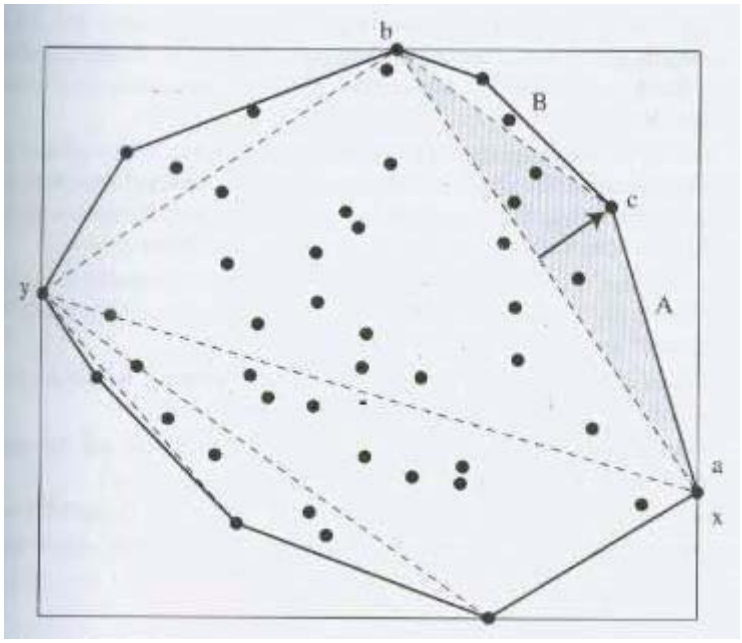

Figure 2. Visual representation of the QuickHull algorithm. To find the entire hull, QuickHull first finds the upper and lower hull using triangulation. The procedure starts with identification of two extreme points (a,b), then a third extreme point c is found directly to the right of ab, and all points inside ∆abc are discarded. The algorithm then recurses on the sides A and B.

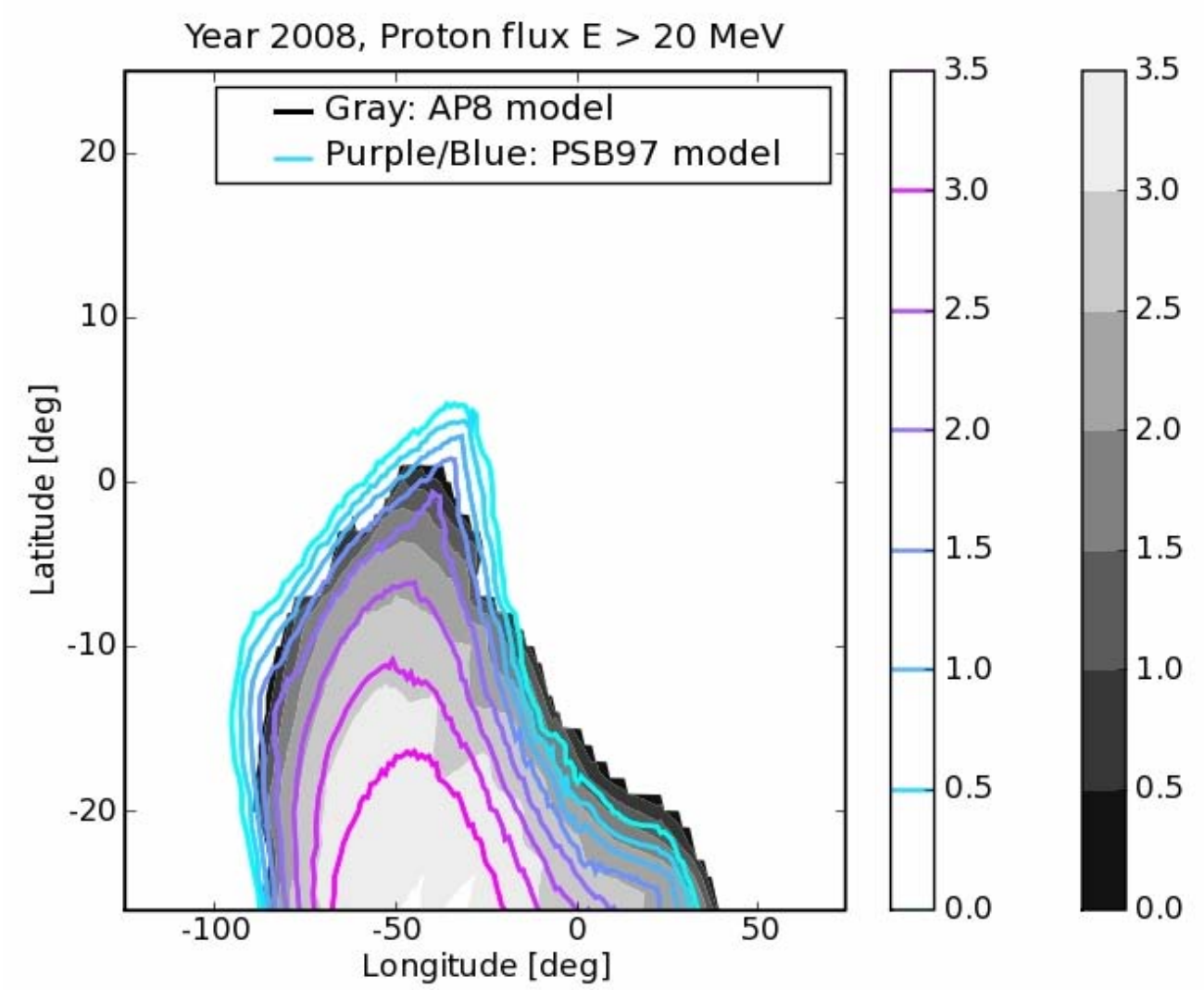

Figure 3. Flux contours for protons with energies E > 20 MeV. The gray shaded region describes proton fluxes as calculated by the AP8 model, the purple/blue contour lines define proton fluxes as attained by the PSB97 model; both show predicted fluxes in 2008. The colorbars on the right side show the mapping between contour lines with $\log_{10}$ flux/ (particles/cm^2 s).

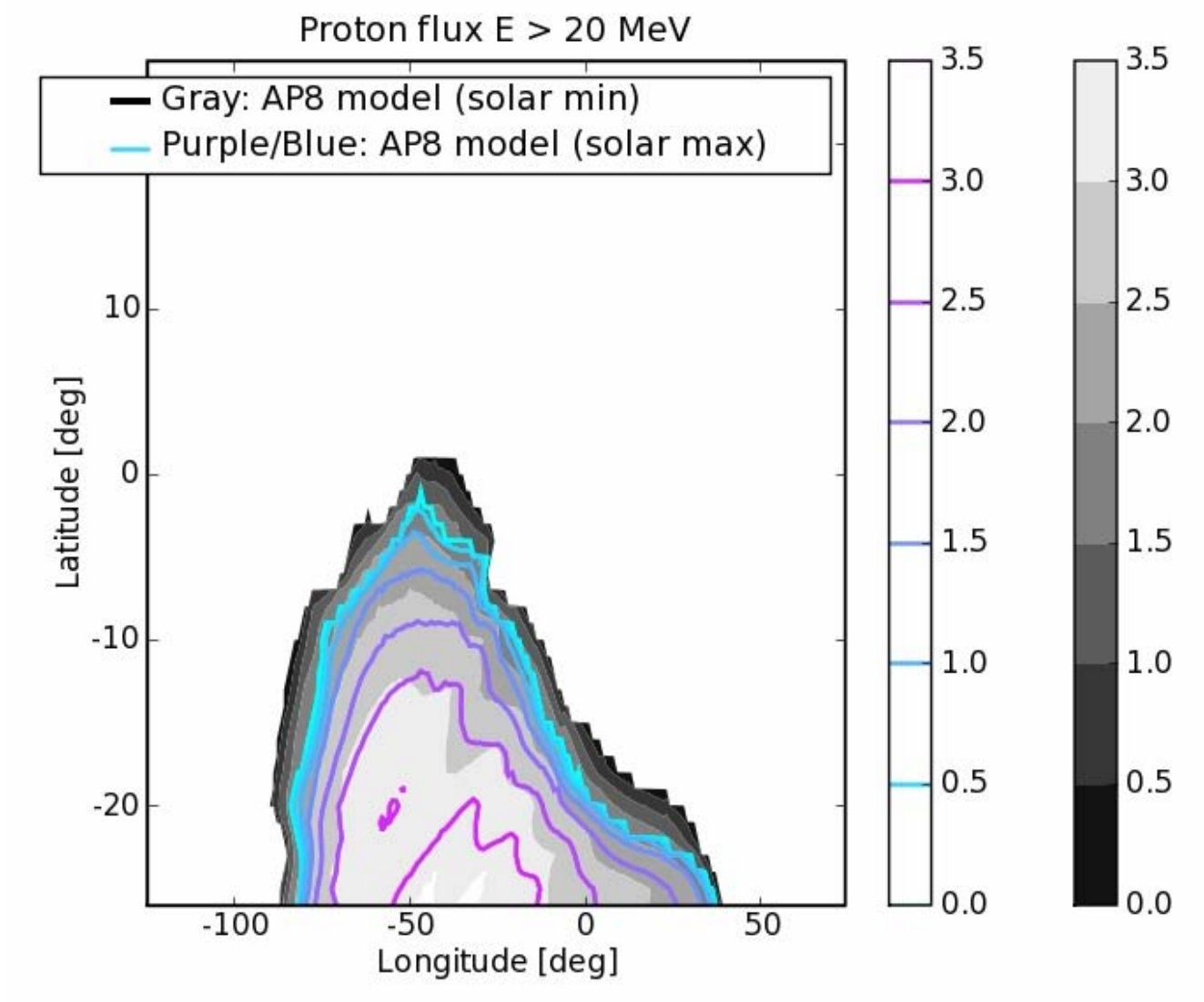

Figure 4. Flux contours for protons with energies E > 20 MeV. The gray shaded region describes proton fluxes of the AP8 model at solar minimum; purple/blue contour lines represent proton fluxes of the AP8 model at solar maximum. The colorbars on the right side show the mapping between contour lines with $\log_{10}$ flux /(particles/cm^2 s).

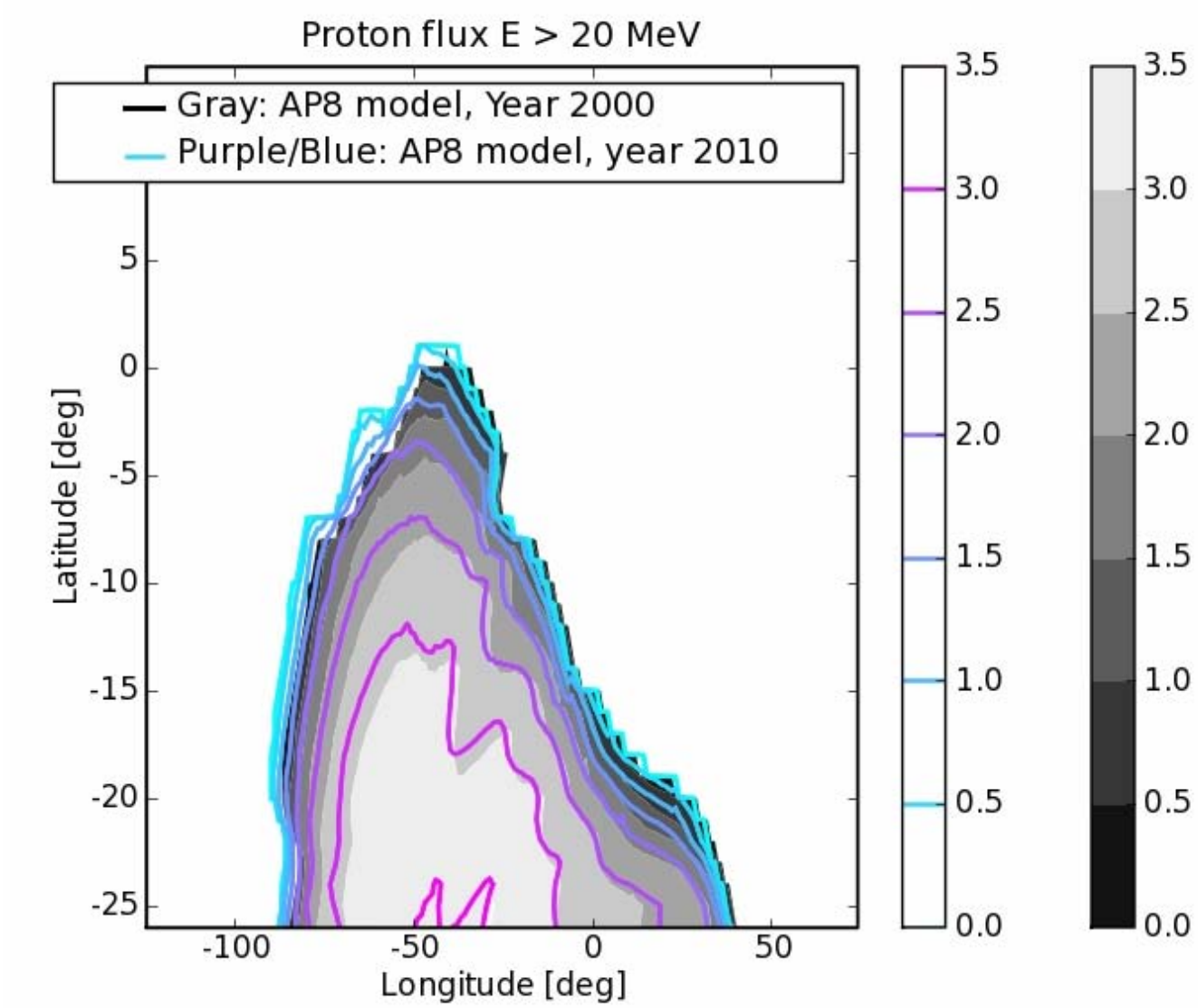

Figure 5. Flux contours for protons with energies E > 20 MeV. The gray shaded region describes proton fluxes of the AP8 model in the year 2000; purple/blue contour lines define proton fluxes of the AP8 model in 2010. The colorbars on the right side show the mapping between contour lines with $\log_{10}$ *flux /(particles/cm*^{2} *s).*

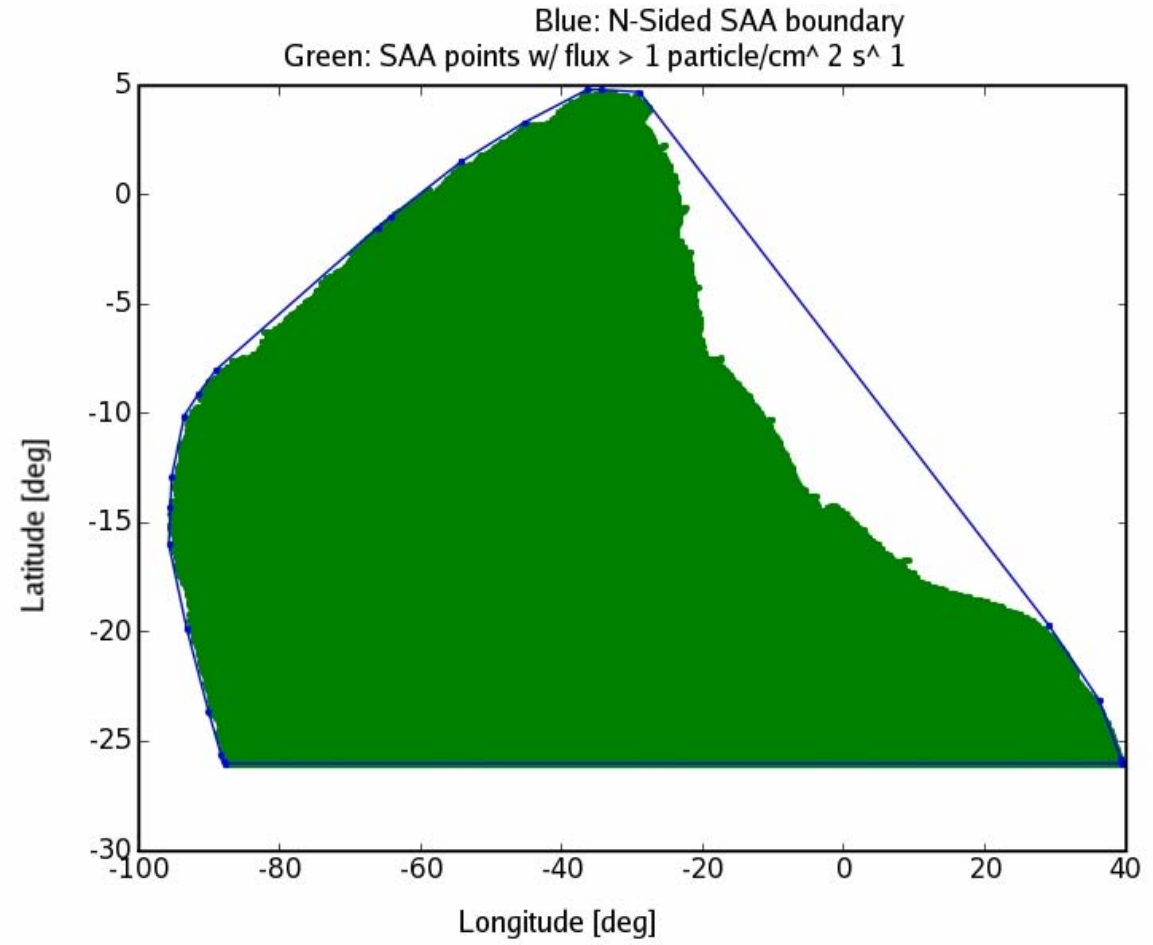

Figure 6. The SAA convex hull with n sides encompassing proton fluxes from both the AP8 and PSB97 models. The green region contains all points where proton fluxes larger than 1 particle/cm^2 s are evaluated on a grid of longitudes and latitudes with 0.1 degree spacing. The blue line shows the convex hull enclosing these points; it is a polygon with 22 edges.

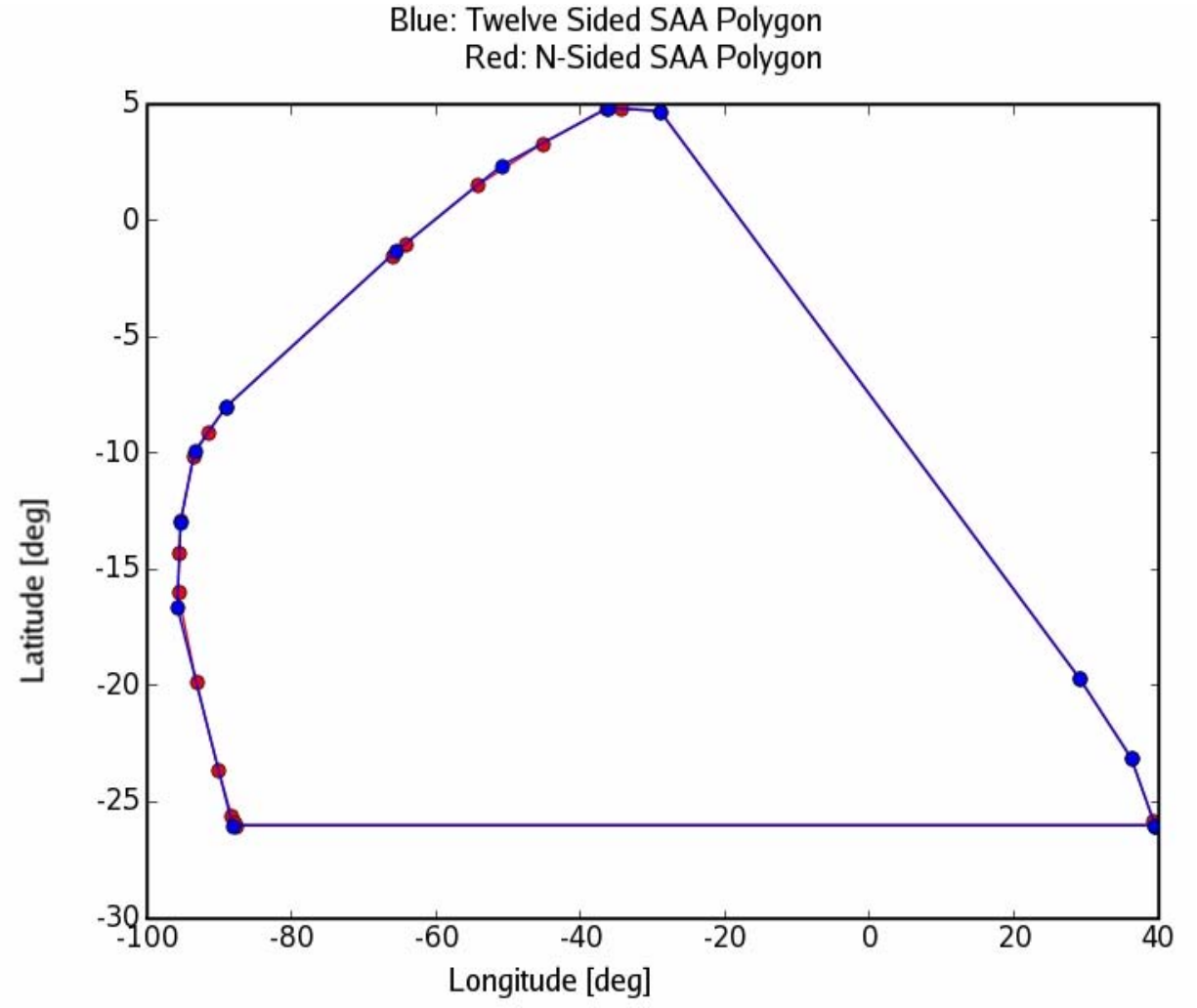

Figure 7. Comparison of the previously attained 22-sided SAA hull with the reduced convex hull of twelve edges. The red boundary is the 22-sided hull, and the blue line defines the minimum area for an SAA polygonal boundary with twelve sides.

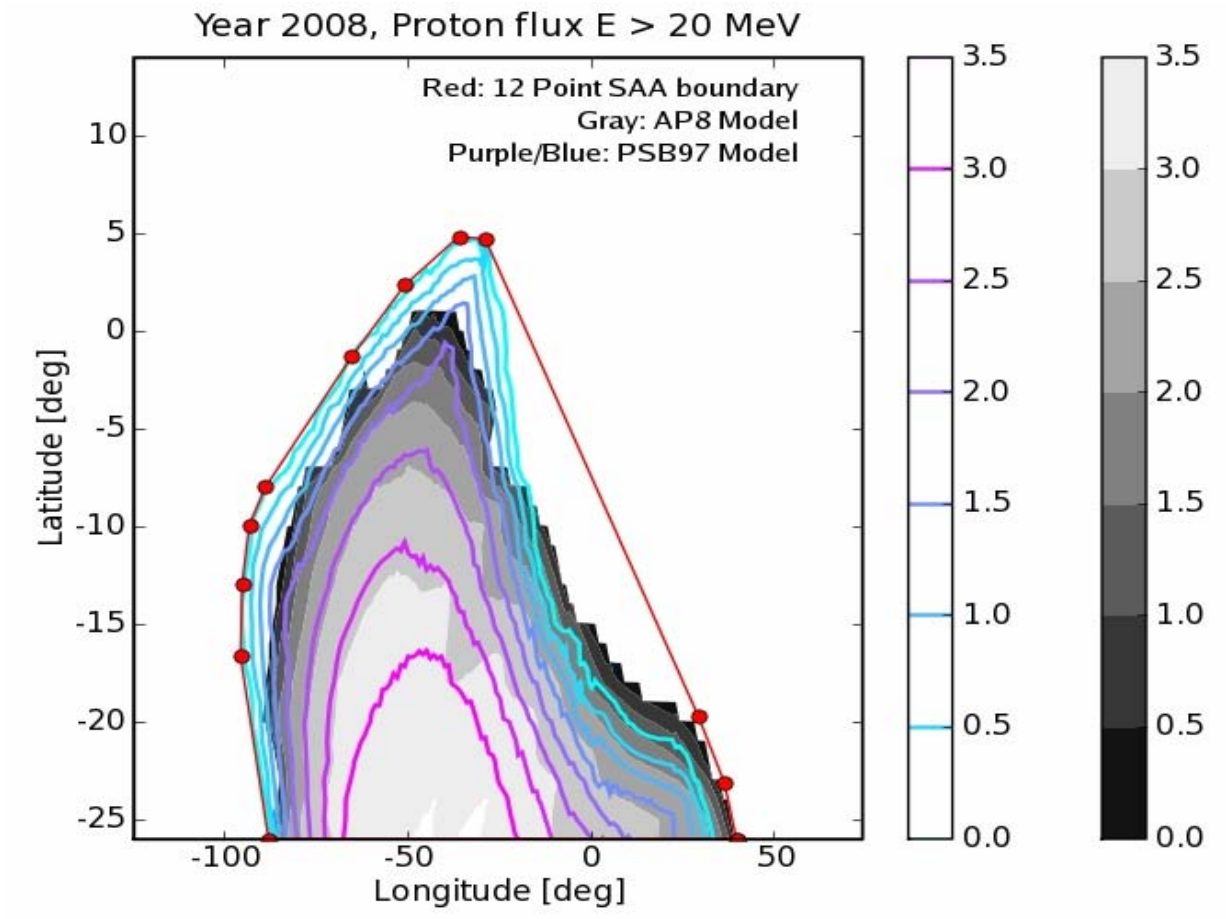

Figure 8. Comparison of the twelve edge SAA boundary with flux contours for protons with energies E > 20 MeV. The gray shaded region describes proton fluxes of the AP8 model, the purple/blue contour lines define proton fluxes of the PSB97 model; both as defined in the year 2008. The colorbars on the right side show the mapping between contour lines with $\log_{10}$ flux /(particles/cm^2 s). The red line shows the twelve sided SAA polygonal boundary of minimal area.

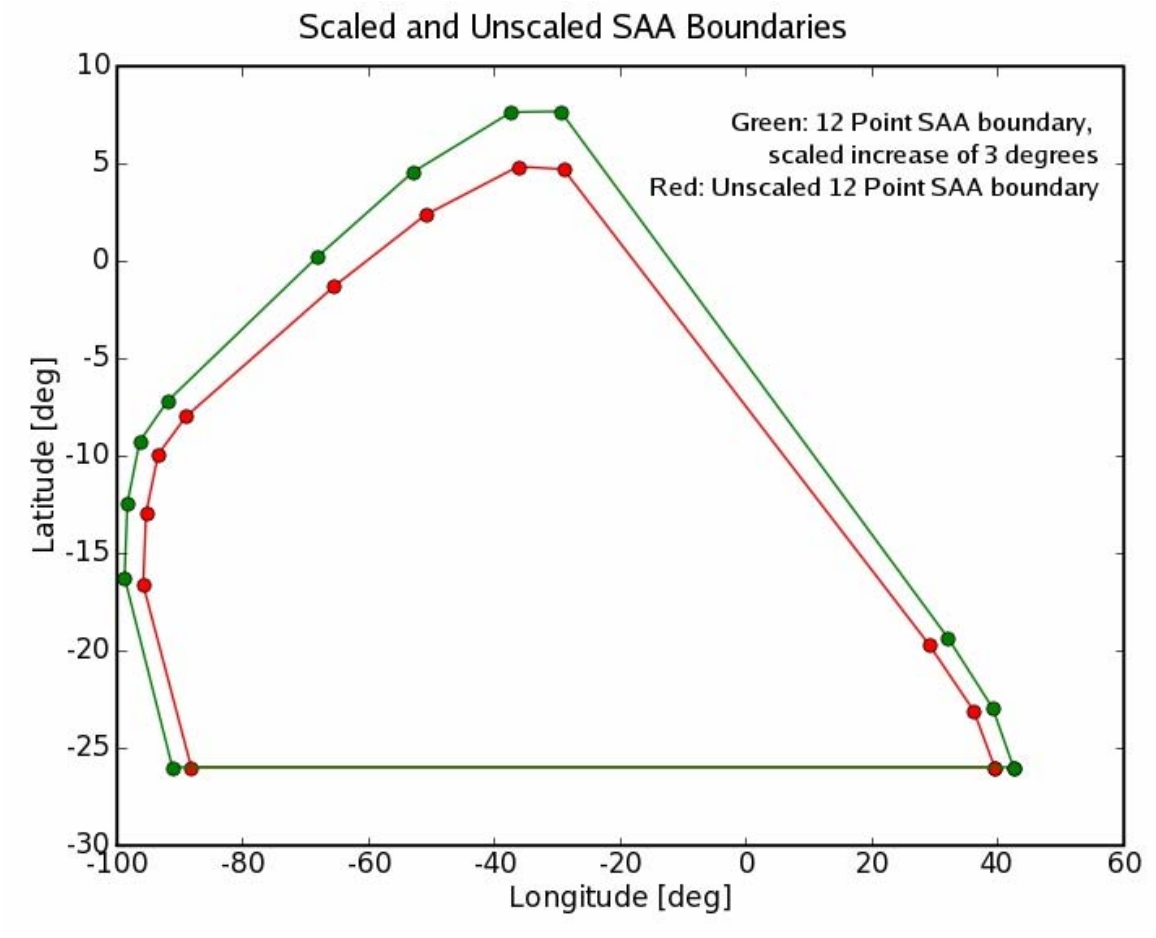

Figure 9. The unscaled twelve sided SAA boundary drawn with a twelve sided boundary scaled with a 3° increase. The red line shows the unscaled boundary, while the green line shows the scaled boundary. The increased hull area represents a safety margin for the twelve sided SAA polygon.

IX. TABLES

Point #	SAA Hull Coordinates	SAA Hull Coordinates (scaled by 1 degree)	SAA Hull Coordinates (scaled by 3 degrees)	SAA Hull Coordinates (scaled by 5 degrees)
1	(39.53, -26.0)	(40.53, -26.0)	(42.53, -26.0)	(44.53, -26.0)
2	(36.19, -23.09)	(37.19, -23.05)	(39.19, -22.96)	(41.19, -22.86)
3	(29.09, -19.69)	(30.09, -19.58)	(32.08, -19.35)	(34.06, -19.11)
4	(-29.00, 4.70)	(-29.15, 5.69)	(-29.45, 7.67)	(-29.76, 9.64)
5	(-36.21, 4.83)	(-36.58, 5.76)	(-37.29, 7.63)	(-38.02, 9.49)
6	(-50.93, 2.35)	(-51.61, 3.08)	(-52.98, 4.54)	(-54.35, 5.99)
7	(-65.45, -1.32)	(-66.31, -0.80)	(-68.03, 0.23)	(-69.7, 1.26)
8	(-89.00, -7.99)	(-89.96, -7.73)	(-91.89, -7.19)	(-93.82, -6.66)
9	(-93.39, -9.93)	(-94.37, -9.71)	(-96.31, -9.25)	(-98.26, -8.79)
10	(-95.34, -12.97)	(-96.33, -12.79)	(-98.29, -12.43)	(-100.26, -12.06)
11	(-95.78, -16.64)	(-96.77, -16.51)	(-98.75, -16.25)	(-100.73, -15.99)
12	(-88.14, -26.0)	(-89.14, -26.0)	(-91.14, -26.0)	(-93.14, -26.0)

Table 1. Twelve coordinate points defining the SAA hull, including coordinates of the SAA hull scaled by an increase of 1°, 3°, and 5°.

Scaled Amount (deg)	Percentage of Lost Observational Area (%)	Percentage of SAA Area Increase (%)
0.5	0.36	2.13
1	0.73	4.29
1.5	1.1	6.47
2	1.48	8.67
2.5	1.86	10.89
3	2.24	13.14
3.5	2.63	15.41
4	3.02	17.7
4.5	3.42	20.02
5	3.82	22.36

Table 2. The percentage of lost observational area and of SAA area increase (with respect to the unscaled area) at various scaling sizes.